Ab Initio Calculations for the Reaction Paths of Levoglucosan: An Intermediate of Cellulose Pyrolysis

Abella, Lorene
Applied Quantum Physics and Nuclear Engineering : Graduate Student

Yamamoto, Keiichiro
MS in Applied Quantum Physics and Nuclear Engineering

Fukuda, Kenji
Institute of Environmental Systems : Professor

Nanbu, Shinkoh
Computing and Communications Center : Associate Professor

他

出版情報：九州大学工学紀要. 66 (2), pp.147-168, 2006-06. 九州大学大学院工学研究院
バージョン：
権利関係：

Memoirs of the Faculty of Engineering, Kyushu University, Vol.66, No.2, June 2006

Ab Initio Calculations for the Reaction Paths of Levoglucosan: An Intermediate of Cellulose Pyrolysis

by

Lorene ABELLA*, Keiichiro YAMAMOTO**, Kenji FUKUDA***,
Shinkoh NANBU†, Noriko OIKAWA††, Koji MORITA‡ and Tatsuya MATSUMOTO‡‡

(Received May 8, 2006)

Abstract

Industrial wood wastes and domestic wastes are composed mostly of cellulose, which is the main constituent in plant materials. Reuse of these products as a biomass energy source is one way of solving the energy problems we are facing today. Studies on the pyrolysis of cellulose reveal that with more than 90 products and by-products, levoglucosan (1,6-anhydro-β-D-glucopyranose) as one of the main products is broken down to produce most of these smaller products. Ab initio calculations were carried out to elucidate the mechanisms of levoglucosan decomposition— an important parameter for char formation that is eyed to be a possible alternative energy source.

Keywords: Cellulose, Levoglucosan, Biomass energy, Ab initio molecular orbital calculations

1. Introduction

Biomass energy comes from a variety of resources available at hand, most of which are animal and domestic wastes and wood products. Conversion of biomass to energy may occur through different processes such as direct combustion, thermal degradation, gasification, methane and ethane fermentation, and so on. Within permissible utilization limits, biomass is one of the most renewable energy resources since they are continuously produced through photosynthesis in plants. Moreover, carbon dioxide emissions evolving from various treatment processes can be countervailed by the carbon neutral effect of trees through reforestation. The net production of forest products corresponds to about 7 to 8 times the world's energy demands, and that by using

* Graduate Student, Applied Quantum Physics and Nuclear Engineering
** MS in Applied Quantum Physics and Nuclear Engineering
*** Professor, Institute of Environmental Systems
† Associate Professor, Computing and Communications Center
†† Contract Researcher, Institute of Environmental Systems
‡ Associate Professor, Institute of Environmental Systems
‡‡ Research Associate, Institute of Environmental Systems

only a small percentage of these resources for energy consumption makes it a good alternative energy resource. Among these sources, wood wastes, which have a cellulose content of ~50%, might be best converted to energy through pyrolysis to yield char, an energy source that can be stored for long periods and less transportation drawbacks, among other dissociation products. Given the appropriate conditions to keep pyrolysis at lower temperatures, char formation is increased while suppressing burning of other volatile components [1]. It has also been observed that flame retardants like metal chlorides [2] and phosphorus-containing compounds effectively increase char yields. Pyrolysis of cellulose and cellulosic materials occur in two ways: depolymerization, the main pathway, and dehydation of cellulose [3] as shown in the scheme below:

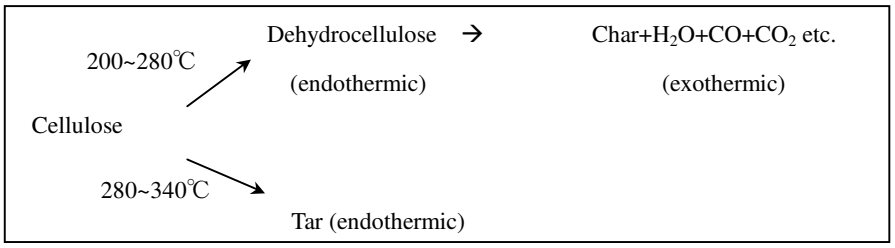

Fig. 1 Depolymerization of cellulose through pyrolysis.

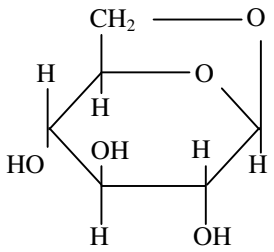

Fig. 2 1,6-anhydro-β-D-glucopyranose (Levoglucosan).

The former occurs at higher temperatures than the latter. This depolymerization process yields 1,6-anhydro-β-D glucopyranose (levoglucosan, **Fig. 2**), a major component of pyrolysis tar and which, when further decomposed, breaks down to furans and other smaller compounds. Although it is widely accepted that the dehydration process is solely responsible for char formation, a notion that char yields can be obtained from the depolymerization pathway by conserving the amount of levoglucosan produced has been suggested [4]. It has also been inferred that the inhibition of levoglucosan polymerization may preclude char formation [5]. This significant role of levoglucosan led to an attempt to further understand its mechanism using the *ab initio* molecular orbital (MO) method [6].

Kato [7] identified eight components of tar from thermal dissociation of cellulose and similar components from that of levoglucosan; see **Table 1** below. At 500˚C, the amount of acetaldehyde increased and made up most of the volatile constituents of tar. Shafizadeh and Lai [8] obtained a 3.9% yield of charcoal from levoglucosan and a much smaller amount from cellulose.

Table 1 Thermal degradation products of cellulose and levoglucosan.

	Cellulose			Levoglucosan		
Compounds	250℃	350℃	500℃	250℃	350℃	500℃
Acetaldehyde	1.8	3.8	11.4	2.2	4.5	20.6
Furan	2.3	2.8	2.6	0.9	0.9	1.1
Propionaldehyde	0.4	0.9	2.6	0.4	0.6	3.2
Acrolein	0.5	1.3	1.9	0.6	0.8	1.4
Acetone	1.1	1.9	4.1	0.9	1.3	3.0
Diacetyl	0.3	0.6	1.6	0.6	1.3	1.2
Furfural	3.7	3.9	3.3	1.9	2.2	1.1
6-Methyl furfural	0.6	0.6	0.6	0.5	0.8	0.5

In reference 8) samples of levoglucosan were prepared in labeled positions as follows: 1,6-anhydro-β-D-glucopyranose-1-^{14}C, -2-^{14}C, and -6-^{14}C. These were pyrolyzed at 600˚C in different environments, namely, in basic catalyst, chloride catalyst, and no catalyst, and in the presence of nitrogen; CO, CO2, and various carbonyl compounds were produced. Tar yields were nearly 50% lesser in acid and chloride catalyzed environments than in non-catalyzed environments; charcoal yields are 7.5 and 4 times much higher in basic and chloride catalyzed environments, respectively. There were 5 proposed schemes by which these products are formed; refer to 17) for details. Pouwels [9] et al found a total of 96 pyrolysis products of cellulose; cleavage and rearrangement of two primary products, levoglucosan and cellobiosan, account for the formation of many smaller products. The abovementioned results were used as a framework and basis of the theoretical approach that is presented in this paper. To understand the mechanism of cellulose pyrolysis focus will be given to levoglucosan depolymerization.

2. Theoretical Method

Ab initio calculations were performed using the Hartree-Fock (HF) [10] and density functional methods with 6-31G(d), STO-3G, and 6-31++G(3df,2pd) as basis sets. The HF theory is simply described by a ground-state N-electron system through a single Slater determinant of the wave function,

$$\left|\Psi_0\right\rangle = \left|\chi_1\chi_2\cdots\chi_N\right\rangle$$

where χ is the spin orbital, and minimizing the energy E to give the best wave function of the functional above,

$$E = \left\langle \Psi_0 \mid H \mid \Psi_0 \right\rangle$$

The Hamiltonian H is defined as [11]

$$H = \sum_i h_i + \frac{1}{2}\sum_{i,j}\frac{e^2}{4\pi\varepsilon_0 r_{ij}}$$

where h_i is the function that describes the kinetic and potential energies of electron i and r_{ij} is the distance between electrons i and j. The HF equation is an eigenvalue equation given by

$$f(i)\chi(\mathbf{x}_i) = \varepsilon\chi(\mathbf{x}_i)$$

and *f(i)*, an effective one-electron operator, is the *Fock* operator of the form

$$f(i) = -\frac{1}{2}\nabla_i^2 - \sum_{A=1}^{M}\frac{Z_A}{r_{iA}} + \upsilon^{HF}(i)$$

where $\upsilon^{HF}(i)$ is the average potential of the electron *i* attributed by the other surrounding electrons. The density functional theory (DFT) differs from conventional ab initio methods such as the HF theory in that its focus is on electron density distribution rather than the many-electron wave function. It also takes into account the electron exchange correlation that describes the depletion of the total density of electrons in a point *r'* due to the presence of an electron in a point *r*; such has not been given attention in the HF theory [12].

Full molecular geometry optimizations were conducted and vibrational frequencies determined using the analytic second derivative method. To improve frequency calculations that use HF/6-31G(d), scaling was adapted using the recommended scale factor of 0.9135 [13]. To find the intrinsic reaction path, an intrinsic reaction coordinate (IRC) [14] analysis was performed. All calculations were carried out using the Gaussian 98 [15] and Gaussian 03W [16] softwares.

3. Results and Discussions

3.1 Molecular geometry optimization of a cellulose fragment model

Molecular geometry optimization of cellulose, having a very high degree of polymerization (about 6000~8000), was done using a fragment model to mimic the entire polymer (see **Fig.3**); HF theory with STO-3G was used. The hydrogen atoms at both ends of the polymer fragment serve to maintain a closed shell structure, thus avoiding ionic and radical structures. In **Table 2**, a comparison of optimization results of this study, those of Arnott and Scott [17] and Gardner and Blackwell [18] obtained through X-ray diffraction is presented. The theoretical values obtained and those through X-ray diffraction are close enough to conclude the validity of the former.

Having a small bond dissociation energy (BDE), cleavage of the glucosidic bond and eventually conversion to low DP cellulose and levoglucosan occur at low thermal dissociation temperatures, or probably at the first stage of cellulose dissociation. All other bonds having larger BDE's than the glycosidic bond do not usually convert to produce gas below 300˚C. In the vicinity of 300˚C, carbon-bonds break to form gaseous products and tar. It is conceivable that the high BDE of the C-H bond restricts H_2 gas production to very small quantities. Dehydration and condensation reactions of the comparatively large cellulose molecule increase carbon ratio and leaves charcoal as a residual product.

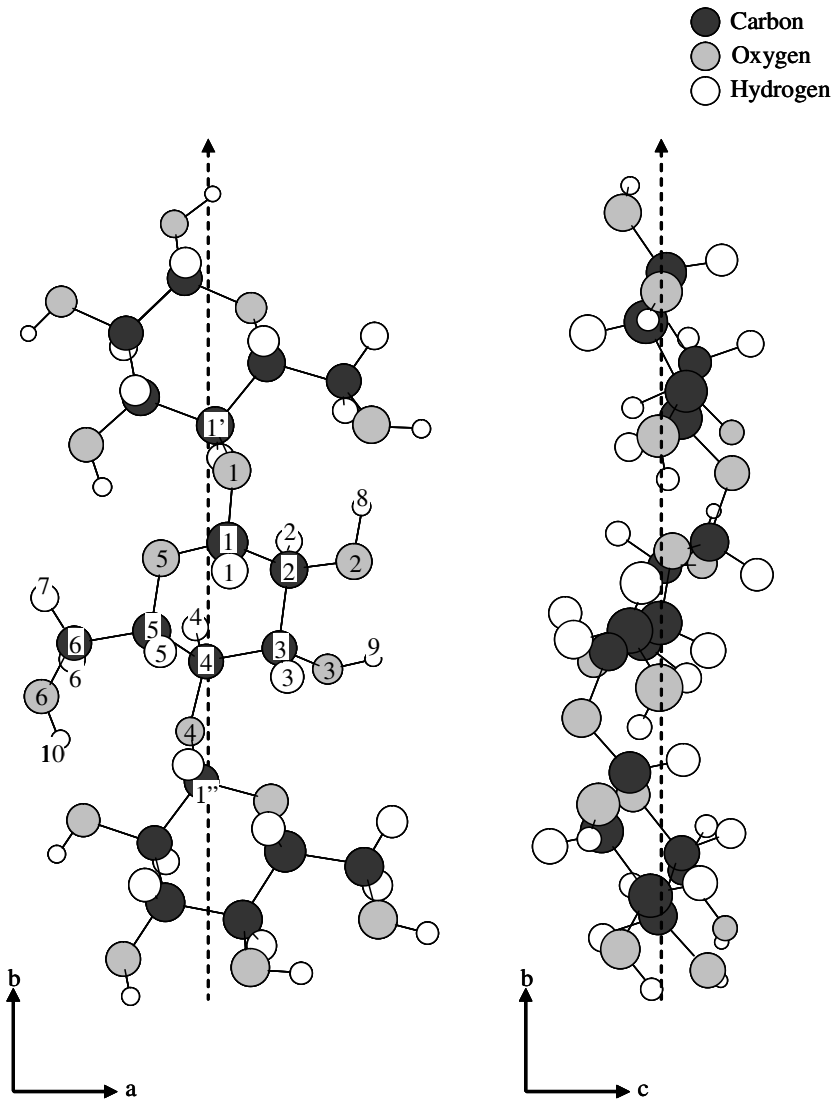

Fig.3 A 3-glucose unit fragment model to mimic cellulose polymer.

Table 2 A comparison of geometry optimization calculations with X-ray diffraction.

Bond Length (Å), Angle (°)		optimization values	Arnott et al	Gardner et al
C-C bond length	C(1)-C(2)	1.571	1.523	1.523
	C(2)-C(3)	1.559	1.521	1.521
	C(3)-C(4)	1.558	1.523	1.523
	C(4)-C(5)	1.571	1.525	1.525
	C(5)-C(6)	1.570	1.514	1.514
C-O bond length	C(1)-O(5)	1.437	1.429	1.429
	C(1)-O(1)	1.429	1.415	1.389
	C(2)-O(2)	1.425	1.423	1.423
	C(3)-O(3)	1.432	1.429	1.429
	C(4)-O(4)	1.438	1.426	1.426
	C(5)-O(5)	1.441	1.436	1.436
	C(6)-O(6)	1.426	1.427	1.427
Bond Angle	C(1)-C(2)-C(3)	109.9	110.5	110.5
	C(2)-C(3)-C(4)	109.1	110.5	110.3
	C(3)-C(4)-C(5)	109.7	110.3	110.2
	C(4)-C(5)-O(5)	109.1	110.0	110.2
	C(5)-O(5)-C(1)	111.0	112.0	112.1
	O(5)-C(1)-C(2)	111.3	109.2	109.3
	O(5)-C(1)-O(1)	109.6	107.3	107.3
	C(1)-C(2)-O(2)	111.9	109.3	109.3
	C(2)-C(3)-O(3)	110.5	109.6	109.6
	C(3)-C(4)-O(4)	115.6	110.4	110.4
	C(4)-C(5)-C(6)	109.0	112.7	112.7
	C(5)-C(6)-O(6)	112.6	111.8	111.8
Dihedral Angle	O(5)-C(1)-C(2)-C(3)	56.1	56.0	-
	C(1)-C(2)-C(3)-C(4)	-51.2	-53.2	-
	C(2)-C(3)-C(4)-C(5)	54.4	53.0	-
	C(3)-C(4)-C(5)-O(5)	-60.6	-55.4	-
	C(4)-C(5)-O(5)-C(1)	65.0	61.1	-
	C(5)-O(5)-C(1)-C(2)	-63.4	-62.2	-

3.2 Levoglucosan reactions and calculations

Figure 4 shows an optimized levoglucosan structure. The pyranose ring in the molecule exists in both the chair and boat conformations. In the former, hydrogen is directed equatorially against the pyranose ring while the hydroxyl base is oriented axially against it; the reverse applies to the latter conformation. Generally, molecules exist in the more stable chair conformation, and a consistent result is shown by the difference in energy with the chair conformation having 2.10kcal/mol less energy than the boat conformation.

3.2.1 Dehydration of levoglucosan

Dehydration of the product levoglucosan in the presence of an acid catalyst is shown in **Fig.5** and one of the main intermediates is glyceraldehyde in tar. IRC calculation results are highlighted in gray. H^+ bonds with the hydroxyl group and the transformation of the hydroxy group to alkyl

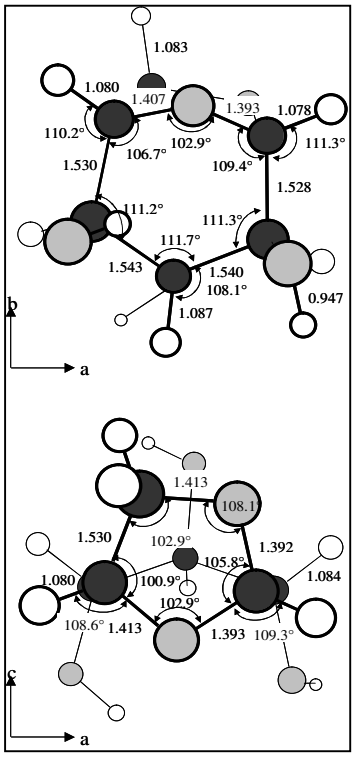

Fig. 4 Optimized levoglucosan structure.

oxonium ion results to Complex1. The distance between C-H_2O^+ lengthens to 2.661Å, which forms a transition structure— about 1.0 Å increase from 1.582 Å of Complex1. Desorption of H_2O leads to Complex 2; desorption of H+ prompts a double C-C bond formation that completes the dehydration process. The structure with a C=C bond is 10.13 kcal/mol more unstable than the one with a C=O, thus with the shift of the double bond an isomerization from C=C to C=O is believed to occur. Such process is illustrated in **Fig. 6**. A single-step isomerization reaction occurs through delocalization of the H and electron of the hydroxyl group. In that event, a four-center transition structure is formed from the hydroxyl group and the C-C bond. Another pathway is the attachment of an H^+ forming a complex; the H^+ cleaved off the OH group. **Figure 7** shows the potential energy curves from dehydration to isomerization of glyceraldehyde. The activation energy of the dehydration process is very small—the ease of procession being largely owed to the presence of the acid catalyst and its collision with H^+.

Because isomerization through H transfer has large activation energy, the reaction was mainly ionic. Furthermore, since complexes 2 and 3 are similar the reaction did not go through C=C but directly to a structure where C=O was formed. Since many species containing a hydroxyl group exist in an intermediate, there is a need to specify the most probable location for dehydration. Glyceraldehyde is a standard compound for isomerization and where other aldehyde isomerizations are compared. Here, the isomerization of glyceraldehyde and 2,3,4-trihydroxybutanal, $C_4H_8O_4$, with the latter as a compound for comparison are considered. The presence of two hydroxyl groups in glyceraldehydes indicates that there are two ways for dehydration to occur; a comparison of the corresponding resulting complexes, products stability, and activation energies are given in **Table 3**. The complex with an H^+ bonding with OH(2) is 4.23 kcal/mol more unstable than the one bonding with OH(3); OH(2) detaches and the structure with a C=C bond more stable by 1.90 kcal/mol. The

activation energy during cleaving off of OH(2) is lower compared to that when OH(3) is cleaved off, thus dehydration of the former is easier to occur. For 2,3,4-trihydroxybutanal, there are three OH groups and four paths of dehydration; a comparison similar to the aforementioned is given in **Table 4**. The complex with the H^+ attaching to OH(4) is very stable, and the OH(2) and H(3) cleave off leaving a stable C(2)=C(3) bond. The low activation energy of the OH(3)-H(2) bond makes it a convenient dehydration point. The following can be visualized from the above-mentioned results: due to electron deficiency of C after desorption of H_2O, electrons can be donated from neighboring C atoms. In this event, since there is only one C atom near the terminal C atom, in comparison to the case where there are two C atoms, electron donation would be difficult, thus leading to a higher activation energy and improbable dehydration. In addition, for carbons attached to aldehyde and carbonyl groups and its neighboring C atoms, even with the presence of two surrounding C atoms the polar character of their functional moieties influences the electrons to favor the O side, and like a terminal C atom, dehydration is less likely to occur. To determine which can be paired with hydrogen for desorption, product stability must be evaluated and the main pathway be assigned to one with highest stability. The same principle applies to cases where there are multiple OH groups present. Whenever there are functional groups surrounding a carbon, an OH group that is not bonded to a terminal carbon should be chosen.

3.2.1a Mechanism (i)

The scission reaction for glyceraldehyde is illustrated in **Fig. 8**; the part that is derived from IRC calculations is highlighted in gray. First, the C-C bond increases, then two carbons and an OH group form four core transition states, and finally the H atom bonds with a C after cleavage. Cleavage of the hydrogen from C-O-H leaves a C=O bond and through the C-C cleavage glyceraldehyde breaks up into formaldehyde and hydroxy-acetaldehyde.

Since the scission reaction is a direct molecular formation mechanism one may associate BDE in the reaction. For this reason, bond dissociation energies, activation energies, and reaction rate constants of glyceraldehyde and 2,3,4-trihydroxybutanal containing structures were calculated and the results listed in **Table 5**. The reaction can be perceived to occur easily due to low activation. To locate the most probable scission point for any intermediate, it is important to determine BDE's and choose one with the smallest value.

In the scission reactions mentioned above, formation of formaldehyde occurs but not CO; see **Fig. 9** for its formation mechanism. Bonding of the H atom from the aldehyde group to its neighboring C atom causes breakage of the C-C bond to form CO. The reaction is a hydrogen transfer as can be seen from the IRC calculation results highlighted in gray; the mechanism is similar to a scission reaction but differs from an ionic reaction. For a molecule bonded to an aldehyde containing or OH-containing C atom, one must determine which occurs first between the C-C bond scission and the CO formation. CO formation, which has low activation energy, takes place more easily than the C-C bond scission.

3.2.1b Mechanism (ii)

A re-evaluation of the C-C scission reaction is made since degradation doesn't occur by using mechanism (i); see **Fig. 10**. The oxygen atoms in both the OH and aldehyde groups have the same orientation; the C-C bond lengthens to 2.110Å at the transition state as the H atom in the OH group delocalizes towards the O atom of the aldehyde group. Further electron delocalizations lead to a formation of an aldehyde and an $HCOH^{2+}$ radical; this scission mechanism is a two-step reaction since it undergoes through two transition structures. A potential energy curve for C-C scissions of hydroxyacetaldehyde (i) and (ii) is shown in **Fig. 11**. C becomes electron deficient as electron

polarization occurs towards O during the OH transition to aldehyde. In the case of glyceraldehydes, instability of the transition state is being alleviated through electron donation from an adjacent carbon. According to calculation results, the activation energies of hydroxyacetaldehyde and glyceraldehyde in mechanism (ii) differ by ~10kcal/mol with the latter being in the higher range.

Figure 12 shows CO (ii) formation from propanedialdehyde, a by-product of levoglucosan decomposition and a standard of derivatization for aldehydes, and used as a comparison to mechanism (i) where hydroxyacetaldehyde decomposed to methanol. H from the aldehyde group delocalizes towards the carbonyl O, gradually increasing the C-C bond length to 1.99 Å at the transition state. From hence, CO and an aldehyde isomer will be formed. Adjunction of H to the aldehyde creates an acetaldehyde isomer. In order for the reaction to take place, the terminal end must contain an aldehyde, whose adjacent C is from a carbonyl group—a condition restricted to reaction (ii). **Figure 13** gives the reaction potential energy curve.

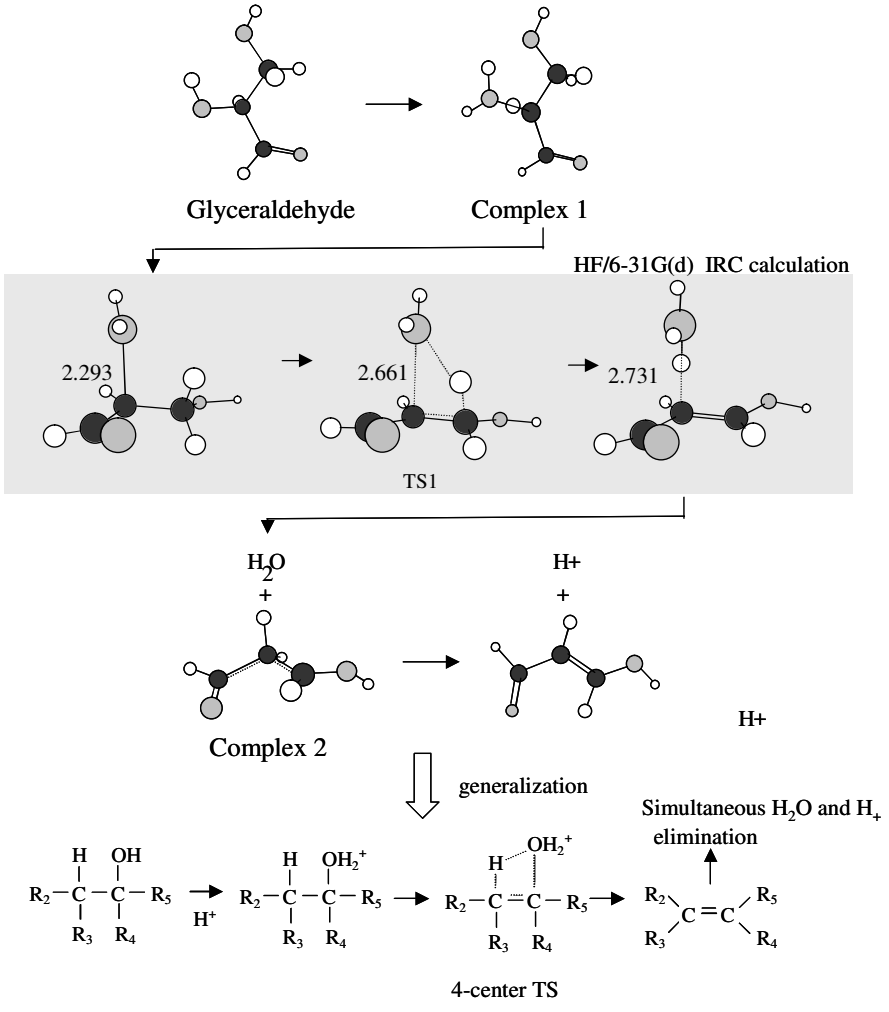

Fig. 5 Acid-catalyzed dehydration reaction.

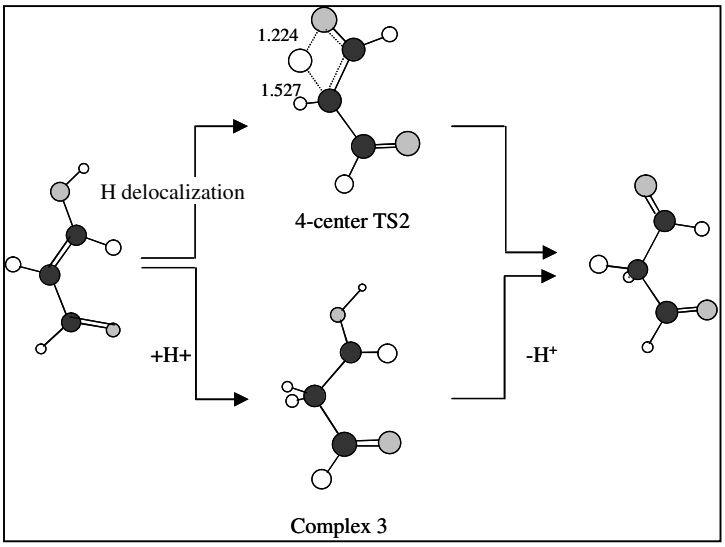

Fig. 6 C=O bond formation from a C=C structure through dehydration.

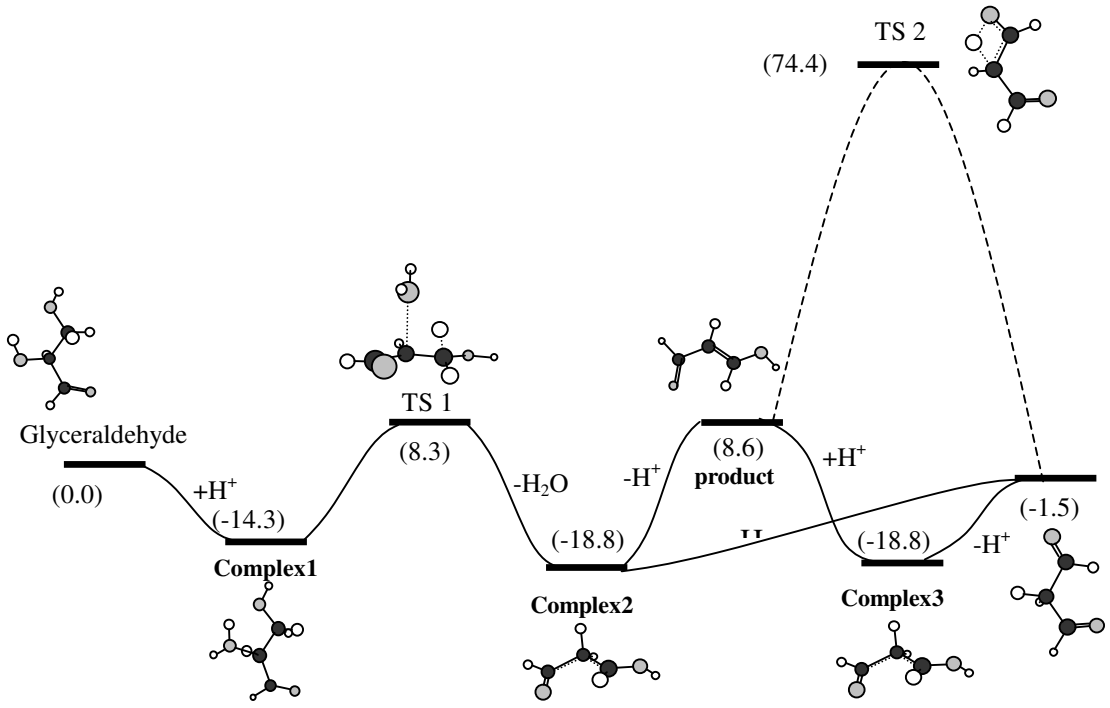

Fig. 7 Potential energy (kcal/mol) profile of the dehydration of glyceraldehyde (HF/6-31G(d)).

Table 3 Energies of products and complexes from dehydration of glyceraldehyde.

	H^+ addition Point	Scission point	Complex 1	Product series	ΔE
C(2)=C(3)	OH(2)	OH(2),H(3)	0.00	0.00	22.64
	OH(3)	OH(3),H(2)	-4.23	1.90	28.80

Table 4 Energies of products and complexes from dehydration of 2,3,4-trihydroxybutanal.

	H+ addition point	Scission pt.	complex 2	Product series	ΔE
C(2)=C(3)	OH(2)	OH(2),H(3)	0.00	0.00	23.23
	OH(3)	OH(3),H(2)	-3.96	4.65	14.23
C(3)=C(4)	OH(3)	OH(3),H(4)	-3.96	11.79	16.69
	OH(4)	OH(4),H(3)	-8.11	2.58	26.14

Note: complex 1, ΔE → HF/6-31G(d) and products →

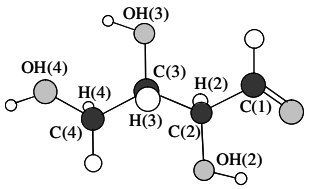

2,3,4-trihydroxybutanal

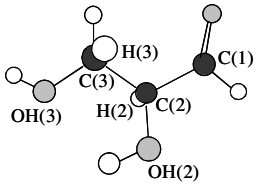

Glyceraldehyde

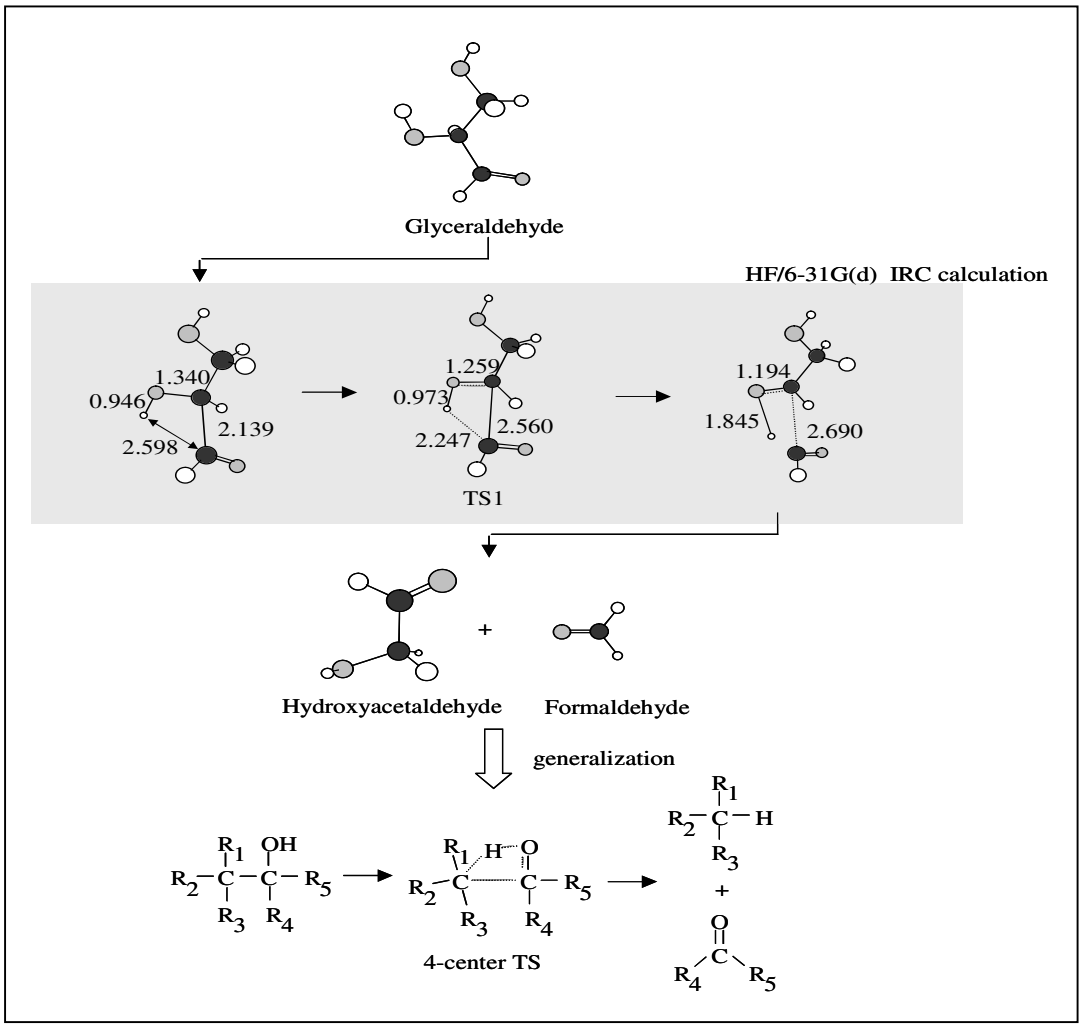

Fig. 8 Mechanism of the C-C bond scission. (i)

Table 5 Bond energies of C-C bond scission.

	bond	C-C bond	O-H bond	ΔE(kcal/mol)
Glyceraldehyde	C(1)-C(2)	75.40	80.31	83.73
	C(2)-C(3)	83.31	80.31	87.72
C4H8O5	C(1)-C(2)	76.88	81.71	85.68
	C(2)-C(3)	79.44	81.71	96.36
	C(3)-C(4)	84.13	81.21	93.69

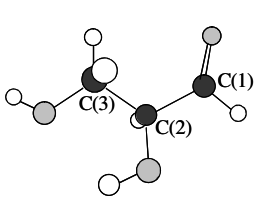

Glyceraldehyde

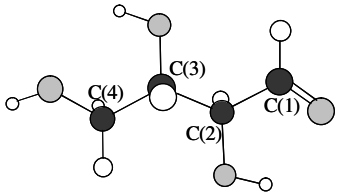

2,3,4-trihydroxybutanal

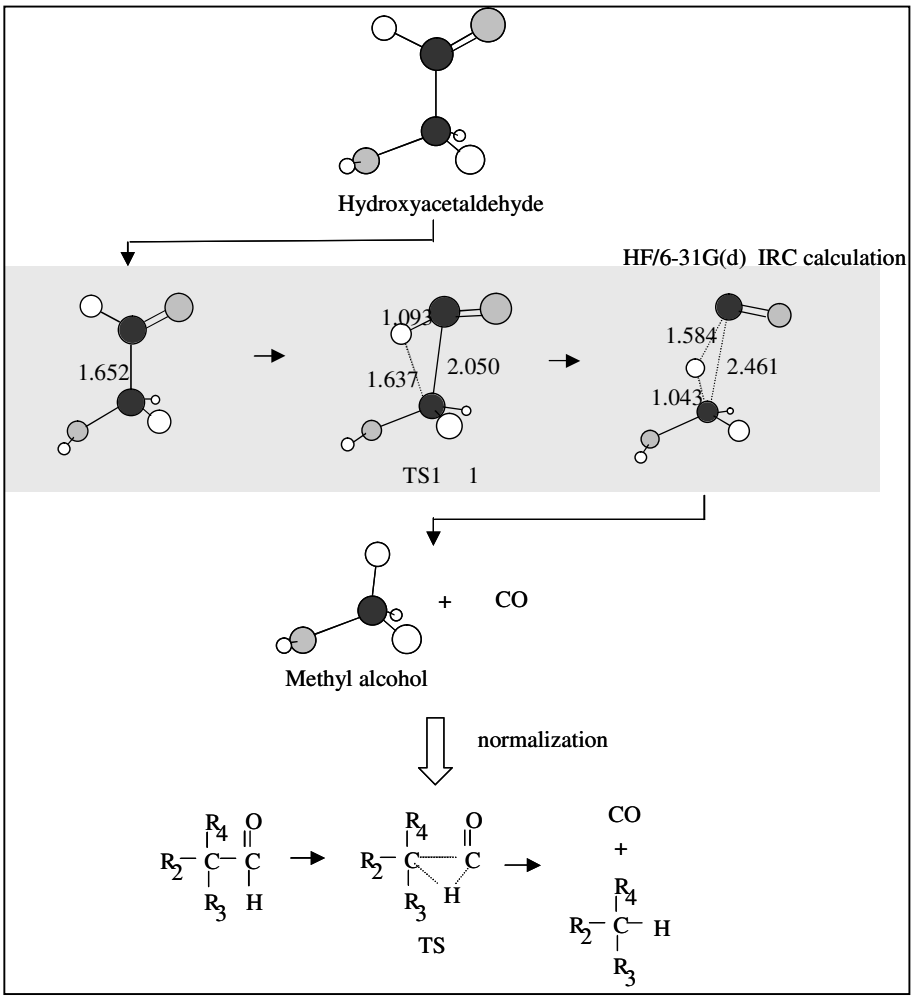

Fig. 9 CO formation reaction (i).

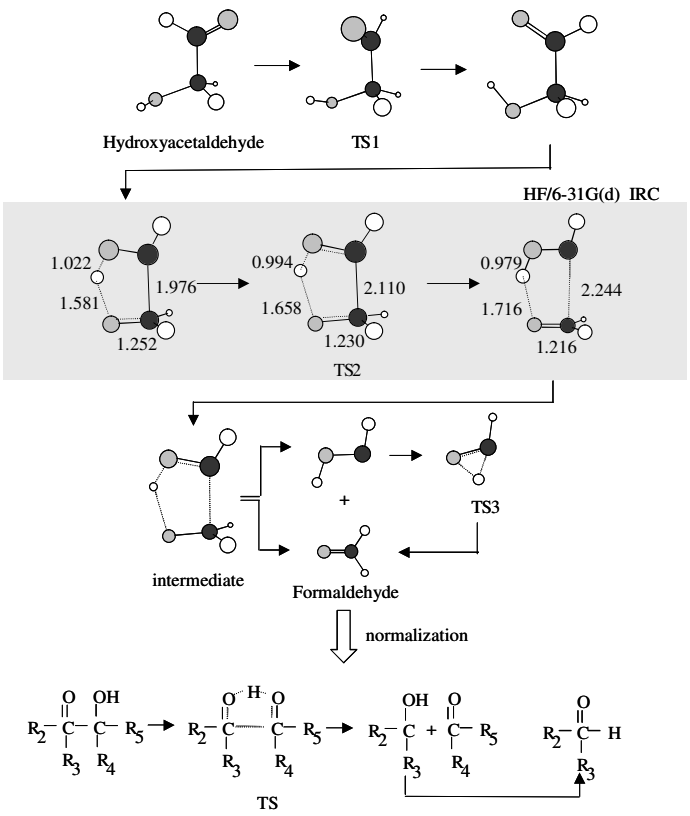

Fig. 10 C-C bond scission. (ii)

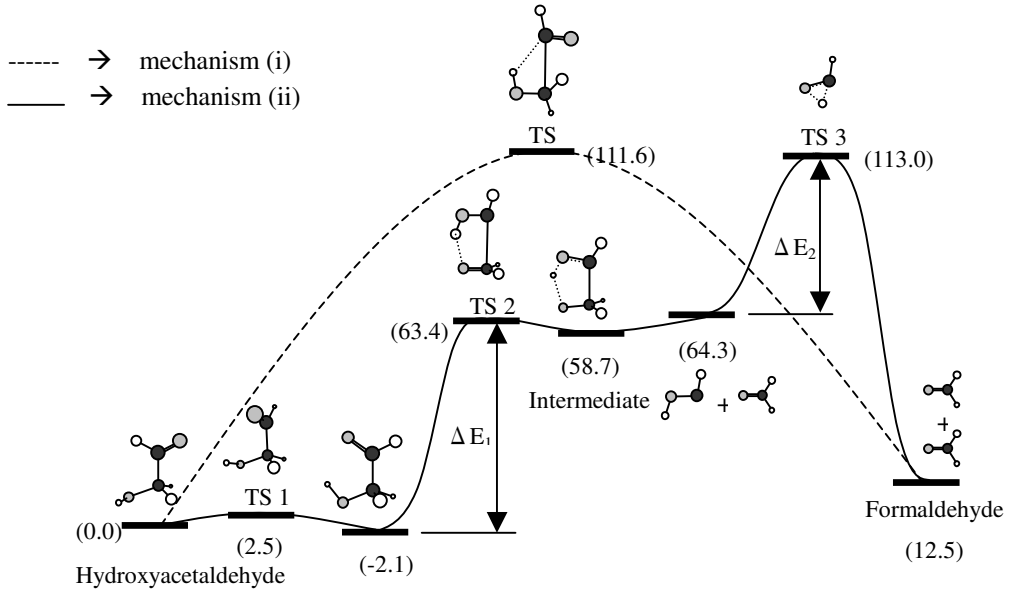

Fig. 11 Potential energy profile of C-C bond scissions (i) and (ii) (B3LYP/6-311++G(3df,2pd)//B3LYP/6-31G(d)).

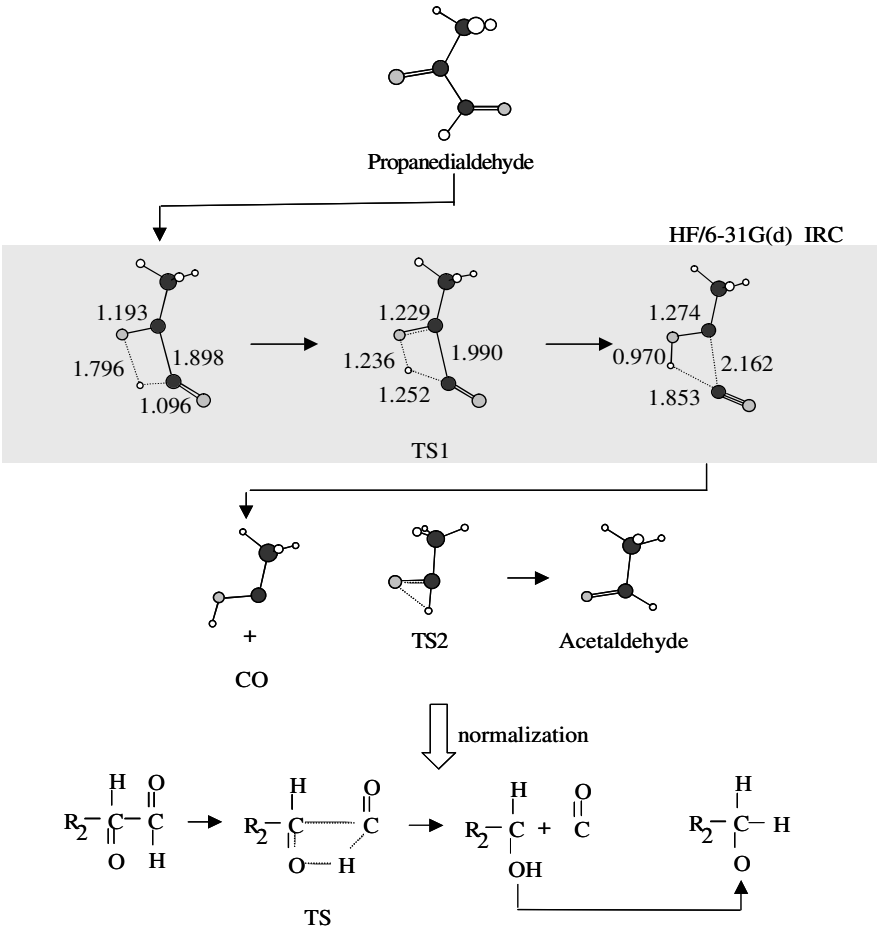

Fig. 12 CO formation reaction (ii).

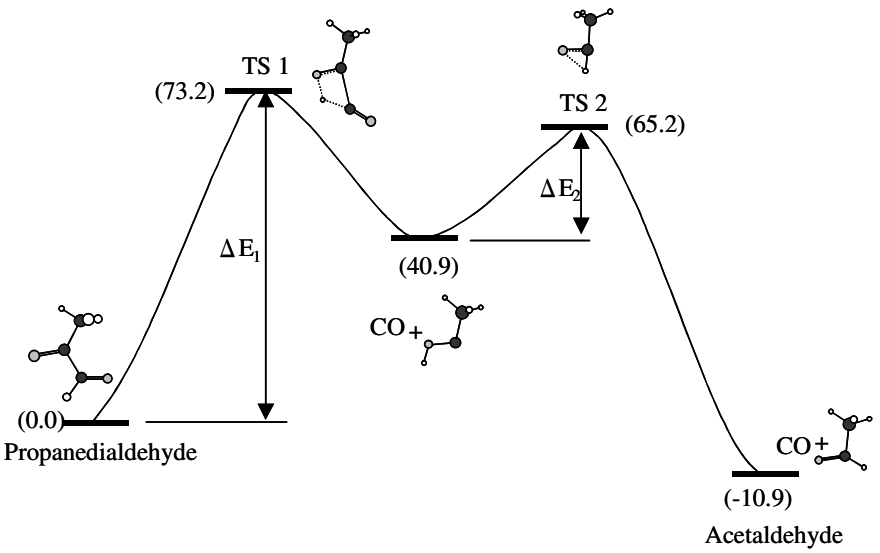

Fig. 13 Potential energy profile of CO formation reaction (ii).

3.2.2 Levoglucosan Hydration

Scission of the very weakly bonded C(1)-O(6) can be considered to occur at the beginning stage of dissociation. However, the C-C bond scission will not be applicable to the aforementioned hydration reaction due to non-bonding of the OH group to C(1). During dissociation of levoglucosan, water vapor that is evolved can be thought to cause hydration, thus can be applied to the C(1)-O(6) bond scission.

The reaction path from levoglucosan to α-D-glucose via hydration is illustrated in **Fig. 14**. The hydration reaction involves scission of a single bond while the one mentioned in section 3.2.1 involved breaking a double bond to form a single bond; the active sites are different for both.

At the initiation step, H^+ attaches to O(6) forming complex1. From the O(6) branching out from the back end of the pyranose ring, H_2O approaches C(1), and at the same time, the length of C(1)-O(6) gradually lengthens to 2.684Å, which is the condition at the transition state. The resulting distance between C(1) and H_2O at this instant is 2.006Å. Moreover, as the distance between C(1)-O(6) increases that of C(1) and H_2O shortens to form complex2. H^+ from H_2O that bonded with C(1) cleaves off and completes the reaction by forming α-D-glucose. C(6) is stable if α-D-glucose is equatorially stretched in the pyranose ring. However, calculation results showed otherwise. The α-D-glucose formed just after hydration is about 6.15 kcal/mol more stable than the one with a C(6) stretched equatorially. This adds to the fact that not all bulky groups in pyranose rings are equatorially directed but only in β-D-glucopyranose are all bulky groups equatorially directed [19]. **Figure 15** illustrates the mechanism of levoglucosan conversion to α-D-glucose. Undergoing 3 transition states, C(6) and the OH group gradually change from the axial to the equatorial conformation and, at the same time, the pyranose ring from the chair to the boat conformation and then back to the chair conformation. Substitution of the OH group attached to C(1) by H in D-glucose, produced two structures: (1) β-D-glucose that is 0.88kcal/mol more stable than (2) α-D-glucose. The stability of the former accounts to its abundance in nature and hence it is beneficial to study its dissociation path.

Potential energies from levoglucosan to β-D-glucose are given in **Fig. 16**. In the dehydration of glyceraldehyde, complexes 1 and 2 have –14.3 and –18.8kcal/mol potential energy, respectively. The complexes formed during the hydration of levoglucosan have lower potential energies with –32.4 and –32.7kcal/mol for complexes 1 and 2, respectively. The activation energies for the latter are also lower. Levoglucosan is formed from a pyranose ring and a five-membered ring containing O; the pyranose ring is thought to give resonance stability to complexes 1 and 2 and the transition structures. The weak C(1)-O(5) bond in the pyranose ring can be easily broken. For the C-C scission reaction, the aldehyde group and OH group must be adjacent. However, since the above condition cannot be met, the C-C bond scission(i) was applied. **Figure 17** shows the process where glucose shifts from a cyclic to a linear structure due to C(1)-O(5) scission. At a 1.765 Å bond length of the latter, a 4-center transition structure is formed, and the OH bonding to C(1) to form an aldehyde completes the reaction. The activation energy of this C(1)-O(5) bond scission is much smaller compared to that of the C-C(i) and (ii) bond scission and CO yielding reaction; for β-D-glucose, the initiation step is the bond scission of C(1)-O(5) producing a linear molecule.

The region where the dehydration and scission reactions in the thermal dissociation of β-D-glucose occur in each intermediate had been sought. Refer to **Figures 18(i)~3.16(iv)**. Through dehydration, release of formaldehyde and CO, and lowering of molecular weight where β-D-glucose changes to 2~6 carbon-tar has been understood. Linearization of β-D-glucose to D-glucose occurs through the C(1)-O(5) bond cleavage, followed by release of an aldehyde and eventually branches to two separate reactions, i.e. another aldehyde cleavage and dehydration. The latter is succeeded by isomerization of the resulting product molecule and a release of CO. The

volume of CO is much lesser than that of formaldehyde since the latter undergoes through multiple generation paths. Formaldehyde generated through dissociation, has a bridged characteristic where it links with other molecules—yields of molecules with more than 6 carbons can be visualized. In thermal dissociation it is suggested that lowering of molecular weights accompanied by polymerization due to the bridged characteristic of formaldehyde may occur.

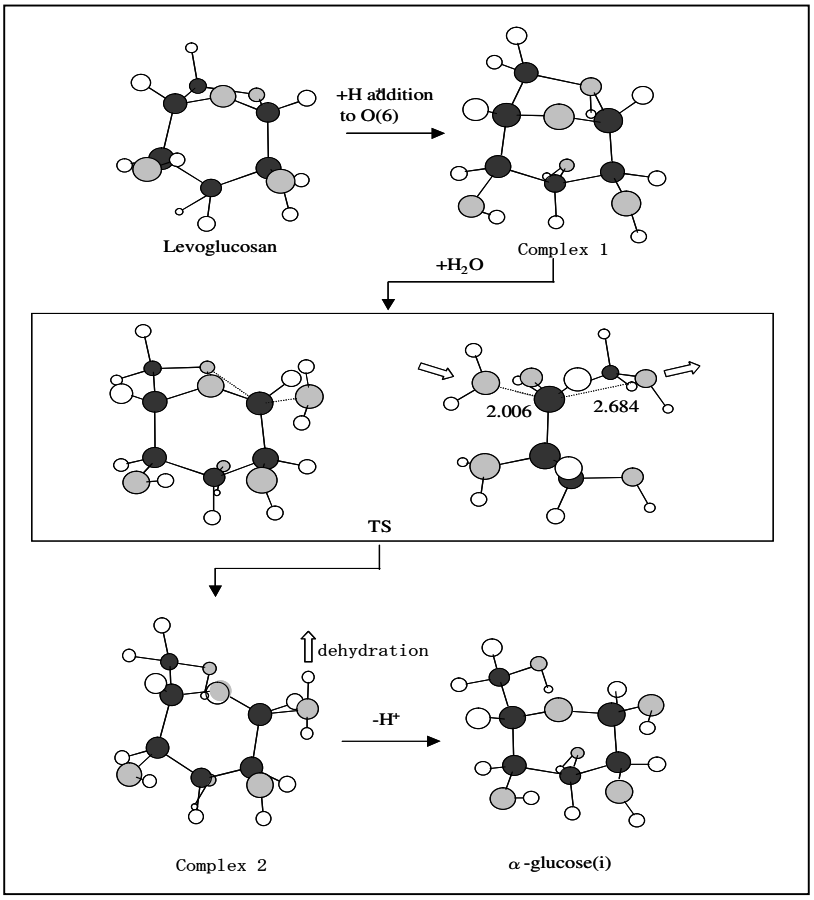

Fig. 14 Reaction mechanism from levoglucosan to α-D-glucose.

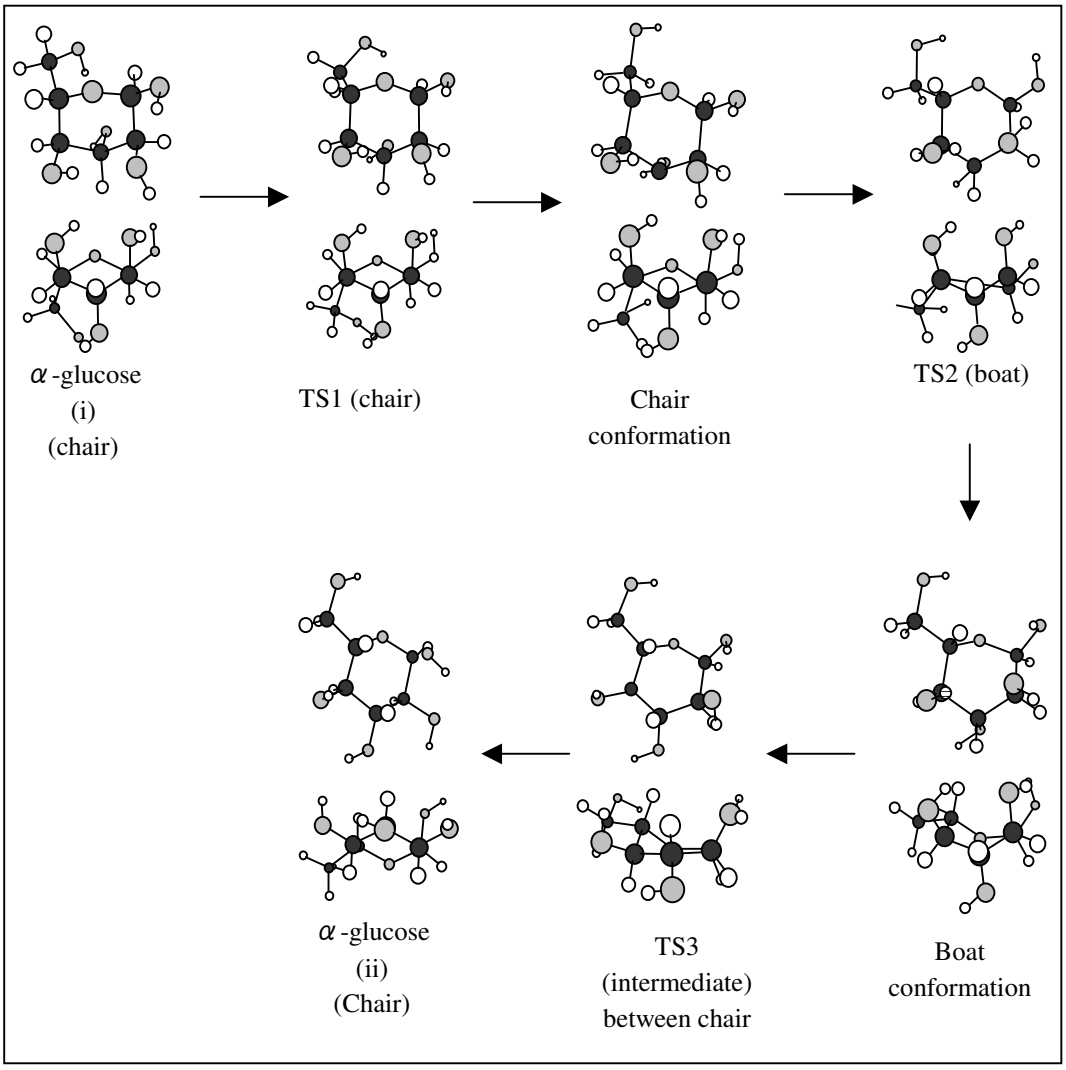

Fig. 15 Mechanism of the conversion of levoglucosan to α-D-glucose.

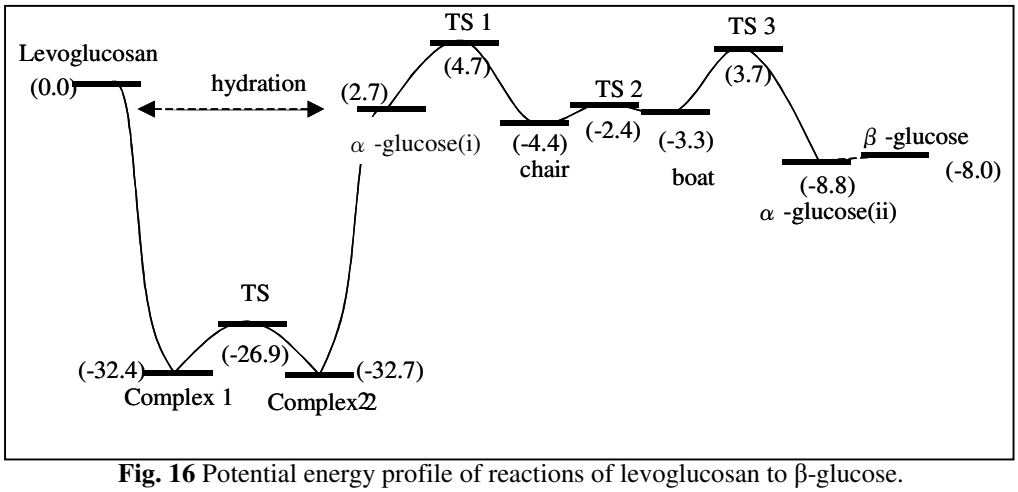

Fig. 16 Potential energy profile of reactions of levoglucosan to β-glucose.

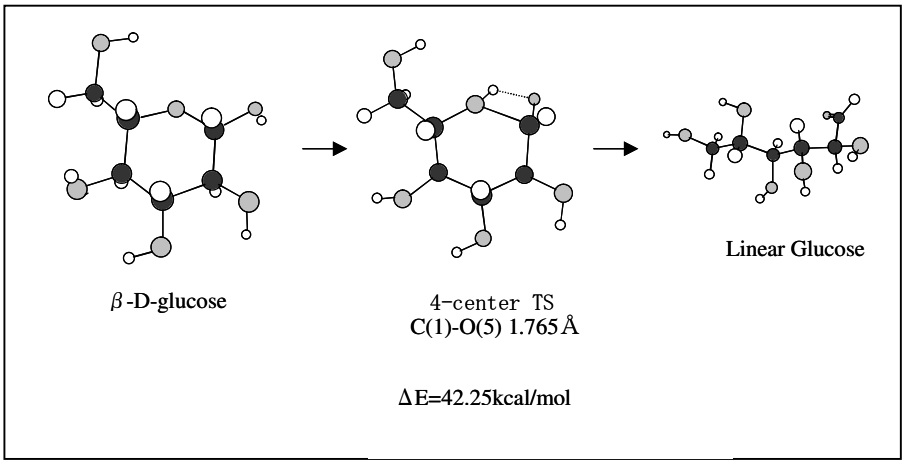

Fig. 17 C(1)-O(5) bond scission of β-D-glucose.

Path (i)

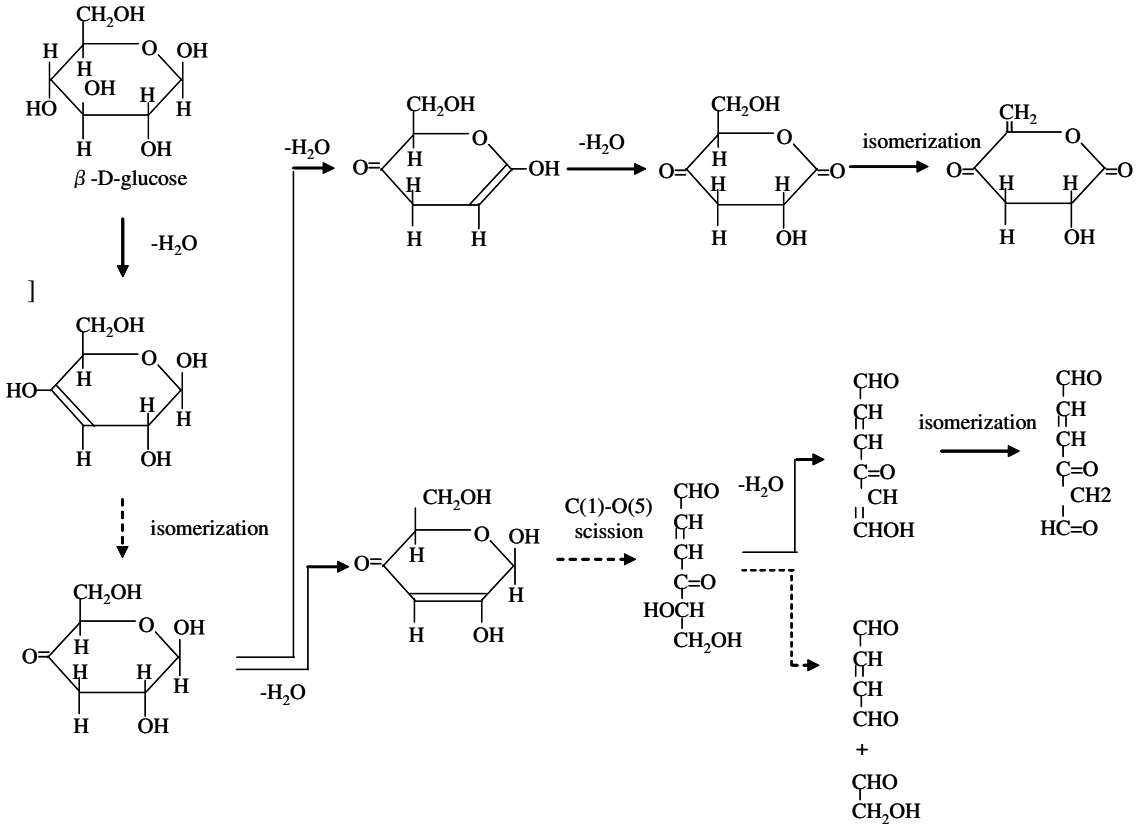

Fig. 18i~iv. Reaction mechanisms of the thermal dissociation of β-D-glucose.

Path (ii)

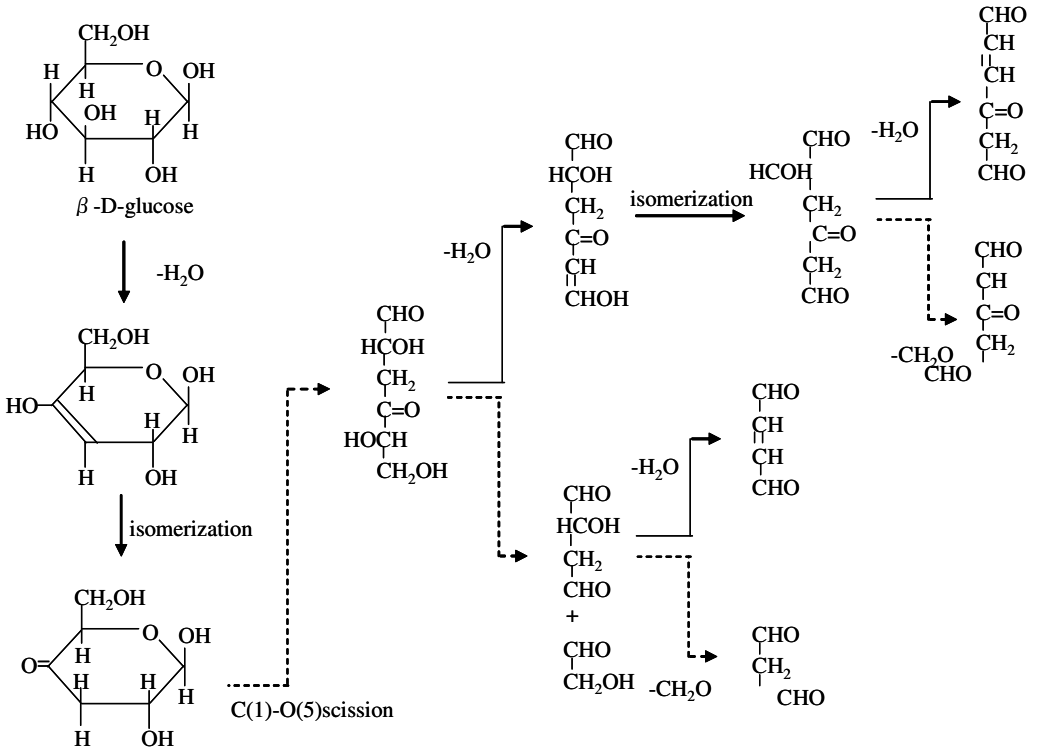

Path (iii)

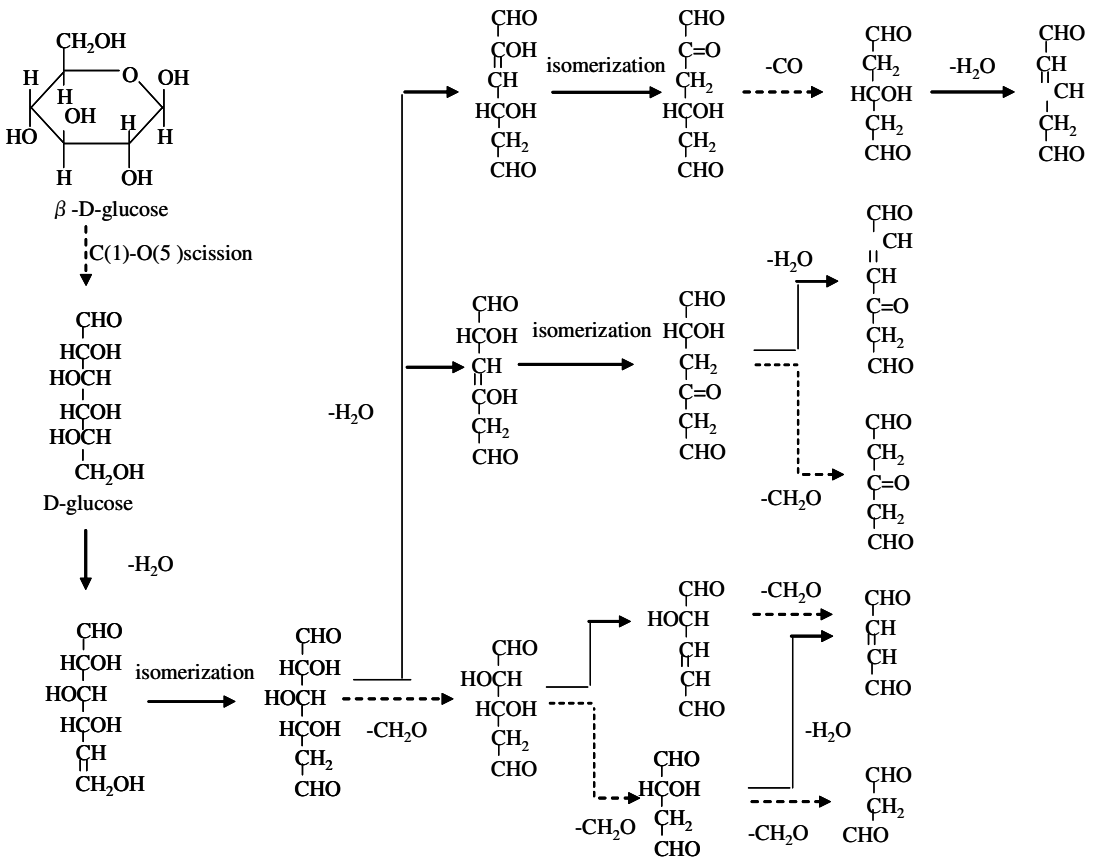

Path (iv)

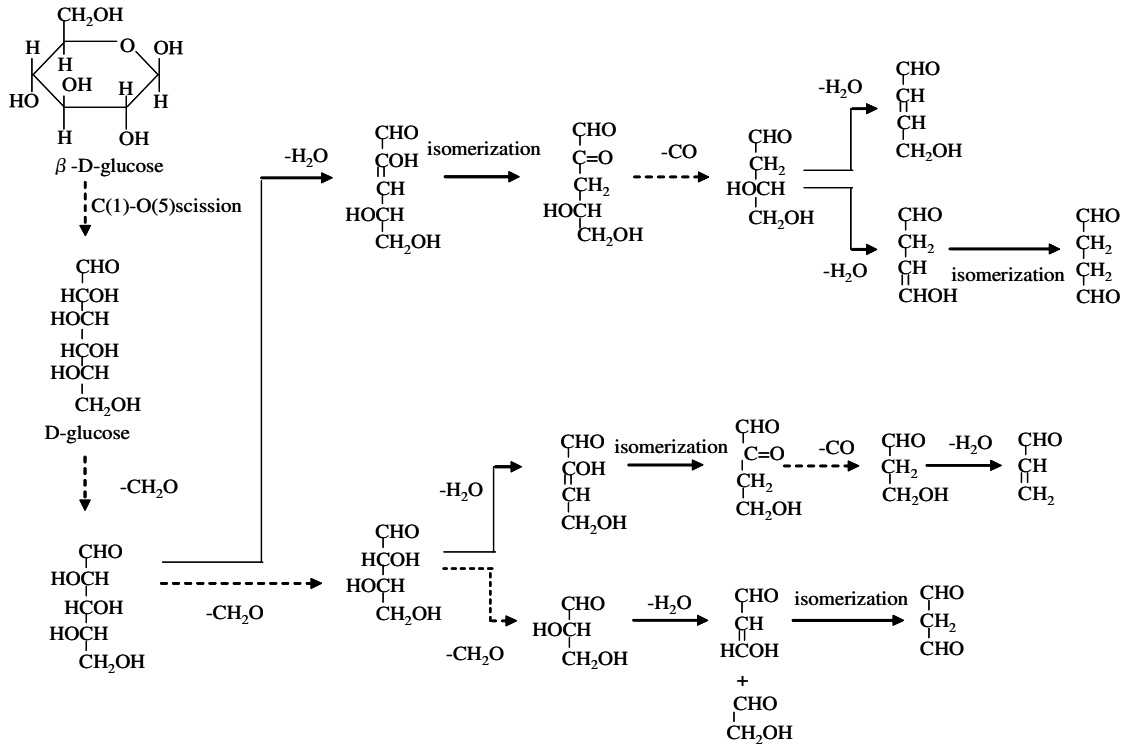

4. Conclusion

The following are deductions from the pyrolysis of cellulose to produce levoglucosan and char through the ab initio molecular orbital calculation results: (1) from the BDE magnitude correlation reduction of the degree of polymerization occurs, and consequently, dehydration due to O-H and C-O scissions; as the reaction progresses, the C-C bond cleaves and further reduction to a lower weight molecule. Pyrolytic reaction mechanisms and dissociation pathways with levoglucosan as the starting molecule have been elucidated and the following information were obtained: (1) dehydration reactions having relatively small activation energies will smoothly occur with an acid catalyst, (2) Reactions that involve a C-C bond scission and CO production occur in 2 steps; the C-C bond cleaves only when an aldehyde group or a carbonyl group coexist with a hydroxyl group, and CO will be evolved only when an aldehyde group is in a close proximity with a carbonyl group, and (3) the formation of an aldehyde suggests lowering of the degree of polymerization and a simultaneous bridged polymerization. Ab initio molecular orbital calculation results are on a par with x-ray diffraction results as given by refs. (15) and (16) though theoretical methods used in this study are in the lower range compared to other ab initio calculation methods. In the calculations that will follow, more rigorous and higher level calculation methods will be used.

References

1) W. D. Ellis, R. M. Rowell, and S. L. LeVan, Thermal Degradation Properties of Wood Reacted with Diethylchlorophosphate or Phenylphosphonic Dichloride as

Potential Flame Retardants, Wood and Fiber Sci., Vol. 19, pp. 439-445 (1987).
2) F. Shafizadeh, Introduction to Pyrolysis of Biomass, J. of Anal. and Appl. Pyrolysis, Vol. 3, pp. 283-305 (1982).
3) F. J. Kilzer, A. Broido; Speculations on the Nature of Cellulose Pyrolysis, Pyrodynamics, Vol. 2, pp.151-163 (1965).
4) S. Soares, G. Caminot, S. Levchik, Comparative study of the thermal decomposition of pure cellulose and pulp paper, Polymer Degradation and Stability, Vol.49, pp. 275-283 (1995).
5) H. Kawamoto , W. Hatanaka, S. Saka; Pyrolysis behavior of levoglucosan as an intermediate in cellulose pyrolysis: polymerization into polysaccharide as a key reaction to carbonized product formation, J Wood Sci., Vol. 49, pp. 469–473 (2003).
6) James B. Foresman, Æleen Frisch, Exploring Chemistry with Electronic Structure Methods, 2nd ed., Gaussian Inc., Pittsburg PA, 302p. (1993).
7) K. Kato; Pyrolysis of Cellulose Part III. Comparative Studies of the Volatile Compounds from Pyrolysates of Cellulose and its Related Compounds, Agr. Biol. Chem., Vol. 31,p. 657 (1967).
8) F. Shafizadeh, Y. Z. Lai; Thermal Degradation of 1,6-Anhydro-β-D-glucopyranose, J. Org. Chem., Vol.37, pp.278- 284 (1972).
9) A.D. Pouwels, G.B. Eijkel, J.J. Boon; Curie-point Pyrolysis Capillary Gas Chromatography High Resolution Mass Spectrometry of Microcrystalline Cellulose", J. Anal. Appl. Pyrolysis., Vol.14, pp.237-280 (1986).
10) A. Zsabo, N. Ostlund, Modern Quantum Chemistry, Dover Publications, Inc., New York, 466p. (1996).
11) P. W. Atkins, R. S. Friedman, Modern Quantum Mechanics, 3rd ed., Oxford Uni. Press, New York, 545p. (1997).
12) W. Kohn, Nobel Lecture: Electronic structure of matter—wave functions and density functionals, Rev.Mod.Phys. Vol. 71, No. 5, pp. 1253-1266 (1999).
13) Database of Frequency Scaling Factors for Electronic Structure Methods, http://comp.chem.umn.edu/database/freq_scale.htm
14) K. Fukui, The Path of Chemical Reactions - The IRC Approach, Accts. Of Chem. Res., Vol. 14, pp. 363-368 (1981).
15) S. Arnott, W. E. Scott; Accurate x-ray analysis of fibrous polysaccharides containing pyranose rings. Part I. The Linked-atom Approach, J. Chem. Soc., Vol.2., pp.324-335 (1972).
16) K. H. Gardner, J. Blackwell; The Structure of Native Cellulose, Biopolymers, Vol.13, pp.1975-2001 (1974).
17) Gaussian 98, Revision A.9, M. J. Frisch, G. W. Trucks, H. B. Schlegel, G. E. Scuseria, M. A. Robb, J. R. Cheeseman, V. G. Zakrzewski, J. A. Montgomery, Jr., R. E. Stratmann, J. C. Burant, S. Dapprich, J. M. Millam, A. D. Daniels, K. N. Kudin, M. C. Strain, O. Farkas, J. Tomasi, V. Barone, M. Cossi, R. Cammi, B. Mennucci, C. Pomelli, C. Adamo, S. Clifford, J. Ochterski, G. A. Petersson, P. Y. Ayala, Q. Cui, K. Morokuma, D. K. Malick, A. D. Rabuck, K. Raghavachari, J. B. Foresman, J. Cioslowski, J. V. Ortiz, A. G. Baboul, B. B. Stefanov, G. Liu, A. Liashenko, P. Piskorz, I. Komaromi, R. Gomperts, R. L. Martin, D. J. Fox, T. Keith, M. A. Al-Laham, C. Y. Peng, A. Nanayakkara, M. Challacombe, P. M. W. Gill, B. Johnson, W. Chen, M. W. Wong, J. L. Andres, C. Gonzalez, M. Head-Gordon, E. S. Replogle, and J. A. Pople, Gaussian, Inc., Pittsburgh PA, 1998
18) Gaussian 03, Revision B.05, M. J. Frisch, G. W. Trucks, H. B. Schlegel, G. E. Scuseria, M. A.

Robb, J. R. Cheeseman, J. A. Montgomery, Jr., T. Vreven, K. N. Kudin, J. C. Burant, J. M. Millam, S. S. Iyengar, J. Tomasi, V. Barone, B. Mennucci, M. Cossi, G. Scalmani, N. Rega, G. A. Petersson, H. Nakatsuji, M. Hada, M. Ehara, K. Toyota, R. Fukuda, J. Hasegawa, M. Ishida, T. Nakajima, Y. Honda, O. Kitao, H. Nakai, M. Klene, X. Li, J. E. Knox, H. P. Hratchian, J. B. Cross, C. Adamo, J. Jaramillo, R. Gomperts, R. E. Stratmann, O. Yazyev, A. J. Austin, R. Cammi, C. Pomelli, J. W. Ochterski, P. Y. Ayala, K. Morokuma, G. A. Voth, P. Salvador, J. J. Dannenberg, V. G. Zakrzewski, S. Dapprich, A. D. Daniels, M. C. Strain, O. Farkas, D. K. Malick, A. D. Rabuck, K. Raghavachari, J. B. Foresman, J. V. Ortiz, Q. Cui, A. G. Baboul, S. Clifford, J. Cioslowski, B. B. Stefanov, G. Liu, A. Liashenko, P. Piskorz, I. Komaromi, R. L. Martin, D. J. Fox, T. Keith, M. A. Al-Laham, C. Y. Peng, A. Nanayakkara, M. Challacombe, P. M. W. Gill, B. Johnson, W. Chen, M. W. Wong, C. Gonzalez, and J. A. Pople, Gaussian, Inc., Pittsburgh PA, 2003.

19) http://www.chemistryexplained.com/Bo-Ce/Carbohydrates.html